MOLECULAR AND CELLULAR BIOLOGY, Nov. 2006, p. 7929–7941 Vol. 26, No. 21
0270-7306/06/$08.00+0 doi:10.1128/MCB.00617-06

Role of Topoisomerase IIβ in the Expression of Developmentally Regulated Genes▽†

Yi Lisa Lyu,[1]* Chao-Po Lin,[1] Anna M. Azarova,[1] Li Cai,[2] James C. Wang,[3] and Leroy F. Liu[1]*

Department of Pharmacology, UMDNJ—Robert Wood Johnson Medical School, 675 Hoes Lane, Piscataway, New Jersey 08854[1]; Department of Biomedical Engineering, Rutgers University, 617 Bowser Road, Piscataway, New Jersey 08854[2]; and Department of Molecular and Cellular Biology, Harvard University, 7 Divinity Avenue, Cambridge, Massachusetts 02138[3]

Received 10 April 2006/Returned for modification 18 May 2006/Accepted 8 August 2006

Mice lacking topoisomerase IIβ (TopIIβ) are known to exhibit a perinatal death phenotype. In the current study, transcription profiles of the brains of wild-type and *top2*β knockout mouse embryos were generated. Surprisingly, only a small number (1 to 4%) of genes were affected in *top2*β knockout embryos. However, the expression of nearly 30% of developmentally regulated genes was either up- or down-regulated. By contrast, the expression of genes encoding general cell growth functions and early differentiation markers was not affected, suggesting that TopIIβ is not required for early differentiation programming but is specifically required for the expression of developmentally regulated genes at later stages of differentiation. Consistent with this notion, immunohistochemical analysis of brain sections showed that TopIIβ and histone deacetylase 2, a known TopIIβ-interacting protein, were preferentially expressed in neurons which are in their later stages of differentiation. Chromatin immunoprecipitation analysis of the developing brains revealed TopIIβ binding to the 5′ region of a number of TopIIβ-sensitive genes. Further studies of a TopIIβ-sensitive gene, *Kcnd2*, revealed the presence of TopIIβ in the transcription unit with major binding near the promoter region. Together, these results support a role of TopIIβ in activation/repression of developmentally regulated genes at late stages of neuronal differentiation.

DNA topoisomerases play important roles in a variety of genetic processes, such as DNA replication, transcription, recombination, chromosome condensation/decondensation, and sister chromatid segregation (51). In mammals, there are two isozymes of DNA topoisomerase II, TopIIα (IIα) and TopIIβ (IIβ) (13). The isozymes share 72% identity in their amino acid sequences. Despite their highly homologous N-terminal ATPase and central core domains, TopII isozymes differ greatly in their C termini (3). In vitro, they possess similar ATP-dependent strand-passing activities, such as catenation/decatenation, knotting/unknotting, and relaxation (2). However, IIα and IIβ are differentially regulated during cell growth and differentiation (6, 47, 49, 52). IIα is only expressed in proliferating cells, with peak expression found at late S and G_2/M phases of the cell cycle (18, 22). IIα is most likely involved in cell cycle events such as DNA replication, chromosome condensation/decondensation, and sister chromatid segregation (8, 10, 12, 20, 21, 50, 53). IIβ, on the other hand, is expressed in all cell types, with elevated expression found in terminally differentiated cells (6, 34, 46, 52). However, the biological function of IIβ is less clear.

Genetic studies employing mouse models have revealed that *top2*β null mutants exhibit a perinatal death phenotype (34, 57). Analysis of the mutant embryos has revealed multiple defects during neuronal development. For example, motor neurons fail to innervate the diaphragm muscle, and the sensory projections are missing in the spinal cord (57). Studies using brain-specific *top2*β knockout mice have demonstrated an aberrant lamination pattern in the developing cerebral cortex and a similar perinatal death phenotype, suggesting an essential role of IIβ in brain development (34). Detailed analysis of corticogenesis has revealed that the migration of postmitotic cortical neurons is affected in *top2*β mutant embryos (34).

The molecular basis for the neuronal migration defect during corticogenesis in *top2*β null embryos is unclear. However, the corticogenesis defect of *top2*β null mutants is similar to that of *reln* mutants (41). The extracellular matrix protein reelin, encoded by *Reln*, is known to be important for neuronal migration during corticogenesis and is found to be down-regulated at both message and protein levels in *top2*β null mutants (34). Down-regulation of reelin could partially explain the abnormal cortical development phenotypes observed in *top2*β mutants. However, the phenotypes of *top2*β deletion seem more complex, since *top2*β knockout mice, unlike *reln* mutant mice, are not viable.

The complex phenotypes of *top2*β null mutants have prompted us to perform a transcription profiling analysis. In the current study, we have compared the gene expression profiles in the brains of *top2*β null and wild-type embryos at three developmental stages. We show that throughout embryonic development of the mouse brain, IIβ is required for the expression of only a subset (1 to 4%) of genes (IIβ-sensitive genes). Expression of genes encoding early differentiation markers and cell growth functions is not altered. However, the expression of about 30% of the developmentally regulated

* Corresponding author. Mailing address: Department of Pharmacology, UMDNJ—Robert Wood Johnson Medical School, 675 Hoes Lane, Piscataway, NJ 08854. Phone: (732) 235-4592. Fax: (732) 235-4073. E-mail for Leroy F. Liu: lliu@umdnj.edu. E-mail for Yi Lisa Lyu: lyuyi@umdnj.edu.

† Supplemental material for this article may be found at http://mcb.asm.org/.

▽ Published ahead of print on 21 August 2006.

genes was affected. The microarray results, together with additional immunohistochemical and chromatin immunoprecipitation (ChIP) analyses, suggest that IIβ may regulate the expression of developmentally regulated genes at late stages of differentiation by controlling chromatin topology.

MATERIALS AND METHODS

Mouse strains. The mouse strains *top2*β$^{+/\Delta1}$ (57) (backcrossed repeatedly with the C57BL/6 strain from the original strain with a mixed genetic background) and *top2*β$^{+/\Delta2}$ (34) (mostly in a 129SvEv background, with a minor contribution from 129SvJ) were used. The *top2*β$^{\Delta1}$ allele (57) contains a neomycin resistance gene that is constitutively expressed, whereas the *top2*β$^{\Delta2}$ allele (34) does not contain any exogenous gene in the truncated *top2*β locus. For timed matings of *top2*β$^{+/\Delta1}$ or *top2*β$^{+/\Delta2}$ mice, the noon time that the vaginal mucus plug was detected was counted as embryonic day 0.5 (E0.5). For the cDNA microarray analysis, total RNAs isolated from the brains of wild-type (wt) and *top2*β$^{\Delta1/\Delta1}$ knockout (ko) littermates were used. For the oligo microarray analysis, total RNAs isolated from the brains of wild-type and *top2*β$^{\Delta2/\Delta2}$ knockout littermates were used.

Total RNA isolation. Embryos were collected by caesarean section at E14.5, E16.5, and E18.5. Whole brains were dissected and immediately immersed into 1 ml of RNAlater solution (Ambion, Inc.) and stored at −20°C until needed for RNA isolation. For total RNA isolation, brain samples were transferred into 500 μl of TRIzol reagent (Invitrogen), and isolation was performed according to the manufacturer's instructions. RNA samples were further purified by using the RNeasy Mini kit (QIAGEN).

cRNA preparation. First-strand cDNAs were generated from 10 μg of total RNA using the SuperScript II reverse transcriptase (RT; Invitrogen). The synthesis was primed by a T7-$(dT)_{24}$ primer: 5′-GGCCAGTGAATTGTAATACG ACTCACTATAGGGAGGCGG-$(dT)_{24}$-3′. Second-strand cDNA synthesis was carried out using the SuperScript Choice system for cDNA synthesis (Invitrogen). cDNAs were then purified by phenol-chloroform–isoamyl alcohol extraction using the phase-lock gel (Brinkman Instrument) and precipitated by the addition of a 0.5 volume of 7.5 M NH_4OAc and 2.5 volumes of 100% ethanol at −20°C. After two washes in 80% ethanol, the air-dried cDNA pellet was dissolved in 12 μl of diethyl pyrocarbonate-treated water. Biotin-labeled cRNAs were synthesized in vitro by T7 RNA polymerase using the RNA transcript labeling kit (Affymetrix). The labeling mixture was purified using the RNeasy Mini kit. cRNAs were eluted from the column with 30 μl of RNase-free water. Twenty micrograms of labeled cRNAs recovered from the elution was fragmented to 35 to 300 nucleotides by incubating in a 40-μl reaction mixture containing 40 mM Tris-acetate (Ac) (pH 8.1), 30 mM MgOAc, and 10 mM KOAc at 94°C for 35 min.

Array hybridization and image scanning. Affymetrix MG_U74Av2 microarrays were hybridized with 15 μg of fragmented cRNAs in 300 μl of morpholineethanesulfonic acid (MES) buffer (0.1 M MES, pH 6.6, 1 M NaCl, 20 mM EDTA, 0.01% Tween 20), with 0.1 mg/ml herring sperm DNA, 0.5 mg/ml acetylated bovine serum albumin (BSA), 50 pM (final concentration) control oligonucleotide B2 (Affymetrix), and eukaryotic hybridization controls *bioB*, *bioC*, *bioD*, and *cre* at 1.5, 5, 25, and 100 pM (final concentrations), respectively. After hybridization, the arrays were washed in buffer A (0.9 M NaCl, 60 mM NaH_2PO_4, pH 7.6, 6 mM EDTA, 0.01% Tween 20), then in buffer B (0.1 M MES, pH 6.6, 0.1 M NaCl, 0.01% Tween 20) on a Fluidics station (Affymetrix), and then stained with buffer C (0.1 M MES, pH 6.6, 1 M NaCl, 0.05% Tween 20, 2 mg/ml BSA) containing 10 μg/ml streptavidin-phycoerythrin (Molecular Probes). Next, the arrays were stained in buffer C containing 0.1 mg/ml normal goat immunoglobulin G (Sigma) and 3 μg/ml biotinylated goat antistreptavidin antibody (Vector Laboratories) and subsequently stained again in buffer C containing 10 μg/ml streptavidin-phycoerythrin. Following the final wash with buffer A, the arrays were scanned by an argon-ion laser with an excitation wavelength of 488 nm and an emission wavelength of 570 nm at a resolution of 3 μm.

Data processing and analysis. The .CEL file (intensity DATA fields) was created from the scanned image by using Microarray Suite 4 (Affymetrix). The .CEL file and the .CDF file (information on the location and identity of different probe cells) were then uploaded into the Rosetta Resolver system for gene expression data analysis (Rosetta Inpharmatics, Inc.). The hybridization intensity analysis and ratio analysis were performed. The Rosetta Resolver application error model for Affymetrix GeneChip microarray data (Rosetta Inpharmatics, Inc.) was used to define and calculate error and *P* values associated with the intensity and ratio data. For intensity analysis, probe sets with *P* values of ≤0.01 were called present. For ratio analysis (Rosetta Resolver System Ratio Builder), probe sets with intensity ratios (either the intensity^{ko}/intensity^{wt} or intensity^{wt}/intensity^{ko} ratio) of ≥1.7-fold and *P* values of ≤0.01 were called differentially expressed. For hierarchical clustering analysis, the normalized absolute expression intensity of each probe set (determined using the Rosetta Resolver application) was analyzed. Cluster and TreeView programs (14) were used to perform one-dimensional hierarchical clustering analysis on the gene expression patterns. A gene heat map plot was generated based on the pair-wise calculations of the Pearson coefficient of normalized expression intensities as measurements of similarity and linkage clustering. The clustered data were loaded into TreeView and displayed by the graded color scheme.

cDNA microarray chip analysis. Total RNA was isolated from the brains of E15.5 *top2*β$^{\Delta1/\Delta1}$ knockout (57) and *Top2*β$^{+/+}$ (wild-type) littermates. mRNA isolation, cDNA generation, array hybridization, and data collection were performed at Incyte Genomics. In brief, fluorescent Cy3- and Cy5-labeled cDNAs were generated from wild-type and *top2*β$^{\Delta1/\Delta1}$ knockout poly(A)$^+$ RNAs, respectively, followed by hybridization to the mouse GEM1 and GEM2 cDNA microarray chips (58). The mouse GEM1 chip contains 7,634 unique genes/clusters (6,357 annotated and 1,277 unannotated), and the mouse GEM2 chip contains 9,514 unique genes/clusters (4,170 annotated). The two-channel intensity data (Cy3 and Cy5) for each array were analyzed using the Rosetta Resolver application. The *P* value assigned to each intensity ratio was defined and calculated using the Rosetta Resolver application error model for Incyte Genomics data (Rosetta Inpharmatics, Inc.). Based on Cy5/Cy3 ratios with *P* values of ≤0.05, genes were called differentially expressed.

RT-PCR. Total RNAs of the whole brains of wild-type and *top2*β$^{\Delta2/\Delta2}$ embryos at different developmental stages were prepared. Total RNAs (0.5 μg each) were used to generate first-strand cDNAs by reverse transcription using the Superscript III RT (Invitrogen). Various cDNAs, including *Gapdh* (GenBank accession no. M32599), *Tubb3* (AW050256), *Neurod1* (U28068), *Gata3* (X55123), *Catna2* (AV353749), *Robo1* (Y17793), *Myt1l* (U86338), *Odz3* (AB025412), *Cdh8* (X95600), *Cacna2d1* (U73487), *Syt1* (D37792), *Alcam* (L25274), *Kcnd2* (AF107780), *Ptgds* (AI840733), *Thy1* (M12379), and *Mef2c* (L13171), were PCR amplified using the following primer pairs: Gapdh-F (5′-AACATCATCCCTG CATCCACTGGT) and Gapdh-R (5′-TGGAAGAGTGGGAGTTGCTGTTG A-3′); Tubb3-F (5′-CCCAAGTGAAGTTGCTCGCAG-3′) and Tubb3-R (5′-A CAGAGCCAAGTGGACTCACAT-3′); Neurod1-F (5′-TCTTTCAAACACG AACCATCCGCC-3′) and Neurod1-R (5′-GATGGCATTAAGCTGGGCACT CAT-3′); Gata3-F (5′-TTATCAAGCCCAAGCGAAGGCTGT-3′) and Gata3-R (5′-ATCTTCCGGTTTCGGGTCTGGATG-3′); Catna2-F (5′-AGTC AACTTTCTACCCACCTCCCA-3′) and Catna2-R (5′-AGACACAACTGGA GAGTTGACAGC-3′), Robo1-F (5′-GCCGAAGGAATATGGCAGAAATG C-3′) and Robo1-R (5′-CGGCAACTTGTCCATTCTGATTGC-3′), Myt1l-F (5′-ACCACAATGGAGAGCAACCTGAAG-3′) and Myt1l-R (5′-AGACCTG AATTCCTCTCACAGCCT-3′); Odz3-F (5′-GACGTTTGGCTTCCATCTGC ACAA-3′) and Odz3-R (5′-TTGCCGATGAGCGACTTGACC-3′); Cdh8-F (5′-ACATCATTCGCTACGACGACGA-3′) and Cdh8-R (5′-GTCCATAGTCCC TTTCTTCAGGCA-3′); Cacna2d1-F (5′-CAAGCGGAACAGACTTCTGATG GT-3′) and Cacna2d1-R (5′-AGTAGGTAGTGTCTGCTGCCAGAT-3′); Syt1-F (5′-ATTCACCTGATGCAGAACGGCAAG-3′) and Syt1-R (5′-ATGT CTGACCAGTGTCGCAGCTCT-3′); Alcam-F (5′-CTGATTGTGGGAATTG TCGTTGGTCTCC-3′) and Alcam-R (5′-TTTCCTCAGGCTATCCAATCCGC T-3′); Kcnd2-F (5′-CACAACAAGGAGTCACCAGCACTT-3′) and Kcnd2-R (5′-GCTGTGGTCACGTAAGGTTGTTCA-3′); Ptgds-F (5′-CCAAGATCAT GGTACTGCAGCCT-3′) and Ptgds-R (5′-TTCTCCTTCAGCTCGTCCTTCA GA-3′); Thy1-F (5′-AGCCAACTTCACCACCAAGGATGA-3′) and Thy1-R (5′-AAATGAAGTCCAGGGCTTGGAGGA-3′).

Quantitative real-time RT-PCR. Quantitative real-time PCR was performed using cDNA generated (see above) in the 7900HT Fast real-time PCR system (PE Applied Biosystems) with the use of SYBR Green. The data were analyzed using the SDS 2.2 software. The threshold cycle (C_T) for each sample was chosen from the linear range. The relative amount of mRNA was calculated with the use of the $2^{-\Delta CT}$ method (32), using *Gapdh* as the normalization standard for each sample. A single PCR product was verified by both its melting temperature and analysis in an agarose gel.

ChIP. Whole brains of TOP2β$^+$ (pool of two *Top2*β$^{+/+}$ and three *top2*β$^{+/\Delta2}$ brains) and *top2*β$^{\Delta2/\Delta2}$ (pool of five brains) embryos were dissected at E18.5 in Dulbecco's modified Eagle's medium (DMEM) (with 10% fetal bovine serum [FBS]). Brain tissues were minced and dislodged to single-cell suspensions in DMEM–10% FBS using an Eppendorf pipette tip. Cells were then filtered through a 100-μm cell strainer. Neutral-buffered formaldehyde was added to a final concentration of 1%, and cells were fixed for 15 min at 4°C. Glycine was then added to a final concentration of 0.125 M to stop the cross-linking reaction, and cells were successively washed in wash buffer 1 (0.25% Triton X-100, 10 mM

EDTA, 0.5 mM EGTA, 10 mM Tris-HCl, pH 8.0), and wash buffer 2 (0.2 M NaCl, 1 mM EDTA, 0.5 mM EGTA, 10 mM Tris-HCl, pH 8.0) and then resuspended in resuspension buffer (1 mM EDTA, 0.5 mM EGTA, 10 mM Tris-HCl, pH 8.0). Chromatin was sheared by sonication to fragments of <4 kb. Chromatin solution was then adjusted to 1× RIPA (50 mM HEPES, pH 7.5, 1% Triton X-100, 0.1% sodium deoxycholate, 0.1% sodium dodecyl sulfate [SDS], 140 mM NaCl, protease inhibitor cocktail [Roche]). Immunoprecipitation (IP) was performed using anti-TopIIβ antibody (Santa Cruz) at 4°C overnight. No antibody was added for the control samples. Protein A-agarose beads were then added to either IIβ IP mixtures or control mixtures to capture IP complexes or serve as controls. The agarose beads were successively washed (twice for each wash) in ChIP lysis buffer (50 mM HEPES, pH 7.5, 140 mM NaCl, 1% Triton X-100, 0.1% sodium deoxycholate, 0.1% SDS, protease inhibitor cocktail), high-salt ChIP lysis buffer (50 mM HEPES, pH 7.5, 500 mM NaCl, 1% Triton X-100, 0.1% sodium deoxycholate, 0.1% SDS, protease inhibitor cocktail), ChIP wash buffer (10 mM Tris-HCl, pH 8.0, 250 mM LiCl, 0.5% NP-40, 0.5% sodium deoxycholate, 1 mM EDTA), and TE (10 mM Tris-HCl, pH 8.0, and 1 mM EDTA). The IP complex was then eluted twice with 75 μl of chromatin elution buffer (50 mM Tris-HCl, pH 8.0, 1% SDS, 10 mM EDTA) at 65°C for 10 min. Supernatants were combined and incubated at 65°C overnight to reverse protein-DNA cross-links. For the input control, 1/100 of the chromatin solution taken for IP was added to 150 μl of elution buffer and incubated at 65°C overnight. After reversal, DNA was purified using the PCR purification kit (QIAGEN). DNA was eluted with 100 μl elution buffer (10 mM Tris-HCl, pH 8.0). For PCR amplification, 1 μl of the elution was used in each reaction mixture. The PCR primers (listed below) were designed to amplify ~200 bp of a DNA sequence located within a 500-bp region upstream of the transcription start site for each gene of interest. The primers were as follows: Myt1l-pF (5′-TGGCCACCTTGTGAGA GACATTCA-3′) and Myt1l-pR (5′-AGATCTGCTTTACCTCCACAGCCA-3′); Cacna2d1-pF (5′-AGTCGGTTGAAGAAGCGACACAGA-3′) and Cacna2d1-pR (5′-AACAGTCAACTCCCAAACCTCCCA-3′); Syt1-pF (5′-GA AAGCCAATTCAGAACGCCATGC-3′) and Syt1-pR (5′-AGGGCTTACATG GTATTGTCGGGA-3′); Cdh8-pF (5′-CATTCCATTGCCAAGTCTCCTGCT-3′) and Cdh8-pR (5′-GGCCCATTGGTCGTGCAAACTTTA-3′); Ptgds-pF (5′-ACCTCCTAGAAGAAGAAACCTCTGCC-3′) and Ptgds-pR (5′-TAGGGCT TGTGAGAAGCAGGTCTT-3′); Kcnd2-pF (5′-ATCTCCGGAGCTACAACA ACAGGT-3′) and Kcnd2-pR (5′-GGCTTCAAACAGGTGTCTTCGCTT-3′); Odz2-pF (5′-GACAAGCAGTGTGGCCTTCACTTT-3′) and Odz2-pR (5′-TC TCCCACTCCAGCAACTGAATGA-3′); Tubb3-pF (5′-TGCACAGAGGTCT CAAGAAGGGTT-3′) and Tubb3-pR (5′-CGCACAATGCGGAGCAAGTCT-3′). To map IIβ binding to the *Kcnd2* gene, sheared chromatin with average sizes of 0.3 kb isolated from the brains of E17.5 TOP2β^{+} (pool of one *Top2*β$^{+/+}$ and three *top2*β$^{+/-}$ brains) and *top2*β$^{\Delta 2/\Delta 2}$ (pool of four brains) embryos were immunoprecipitated using anti-IIβ antibody. DNAs isolated from the ChIP assay was screened for IIβ binding using the following primer sets: −19.6KbF (5′-A GTGTCTCAAATCATCTATGCTTGTCT-3′) and −19.6KbR (5′-GGAGAGG TGTAGTTCAGTTGGTA-3′); −5KbF (5′-CGTTGTAGACCAGTAGTGAGT GTAGG-3′) and −5KbR (5′-ATTGGACTGGGATCCAGTTAGTGC-3′); −2.5KbF (5′-ACAGCAAATCACAACCCACTTTCC-3′) and −2.5KbR (5′-AG TGGAGTTCACTAGAAAGAGCAGAC-3′); Kcnd2-pF (see above) and Kcnd2-pR (see above); +2.5KbF (5′-GAAGCCTCCCATATCTTTGAGGGTG TA-3′) and + 2.5KbR (5′-ACGACCAGCAGAATAAAGGGAATGAAGG-3′); +10KbF (5′-CCAGTTTGGAAGGAGTTCTGTGGA-3′) and + 10KbR (5′-AGTCTGAAGCATTCTGGGTAAGGG-3′); +503.55KbF (5′-AAATCCA AAGGATGGACAGGGAGG-3′) and + 503.55KbR (5′-CCTGTTGAAATGA CAAGCATGTTGGG-3′). These primer sets were used for the amplification of DNA sequences located at kb −19.6, −5, −2.5, −0.5, +2.5, +10, and +503.55 of the *Kcnd2* gene, respectively.

Immunohistochemical analysis. Brains of E18.5 embryos and whole heads of E14.5 embryos were dissected and fixed by soaking overnight in phosphate-buffered saline (PBS) plus 4% paraformaldehyde at 4°C. After washing with ice-cold PBS for 1 h, the specimens were separately processed for paraffin embedding or cryoprotection in OCT compound (Sigma). Tissues embedded in paraffin blocks were sectioned to 6-μm slices for mounting on SuperFrost Plus slides (Fisher). Sections were dewaxed by soaking in xylene (twice for 5 min) and rehydrated by soaking in ethanol with a decreasing percentage (5 min, two times each) and then in H_2O for 3 min. Tissue sections were then treated with 3% H_2O_2 for 10 min, followed by rinsing twice in PBS and then incubation in ADB solution (0.05% Triton X-100, 10% goat serum, and 3% BSA in PBS) for 30 min. Rabbit anti-histone deacetylase 2 (HDAC2) antibody (1:100 dilution, in ADB; Santa Cruz Biotechnology) was applied to the sections, and incubation was continued for 2 h. After four washes (5 min each) in TBST (Tris-buffered saline plus 0.1% Tween 20), sections were incubated with horseradish peroxidase-conjugated goat anti-rabbit secondary antibody (diluted 1:500 in ADB; Chemicon) for 45 min. After being washed four times (5 min each) in TBST, tissue sections were incubated with 3-3′ diaminobenzidine tetrahydrochloride working solution (Vector Laboratories, Inc.) for 5 min, followed by rinsing in H_2O, dehydrating, and mounting. Images were visualized under a microscope and captured with a charge-coupled-device camera. For cryosection analysis, cryosections (16 to 20 μm) were fixed in PBS containing 4% paraformaldehyde for 10 min. After four washings in PBS (2 min each), cryosections were incubated in ADB solution for 30 min and then incubated with either rabbit anti-HDAC2 antibody or rabbit anti-TopIIβ 779 antibody (obtained from F. Boege, University of Wurzburg, Wurzburg, Germany) in a humidified chamber at 4°C overnight. After four washes (5 min each) in TBST, the slides were incubated for 30 min at 37°C with the Cy3-conjugated goat anti-rabbit secondary antibodies (Jackson ImmunoResearch). After washing in TBST (four times, 5 min each), the slides were mounted with Gel/Mount (Biomeda Corp.). For coimmunostaining of IIβ and HDAC2, rabbit anti-IIβ (Santa Cruz) and mouse anti-HDAC2 (Upstate) antibodies were used, followed by secondary staining with Cy3-conjugated goat anti-rabbit and Cy2-conjugated goat anti-mouse secondary antibodies. Images were visualized under a fluorescence microscope and photographed with a charge-coupled-device camera.

Microarray data accession number. The complete microarray data set has been deposited in the NCBI Gene Expression Omnibus database (http://www

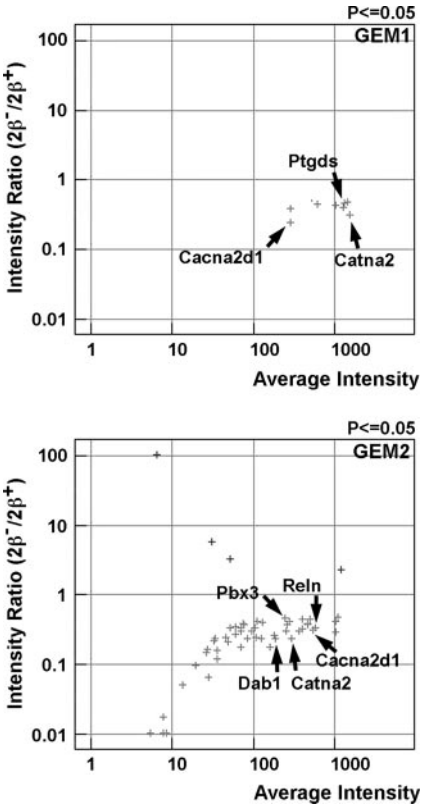

FIG. 1. Transcription profiling of the brain of a *top2*β$^{\Delta 1/\Delta 1}$ mutant embryo by using cDNA microarrays. Total RNAs isolated from the brains of E15.5 *top2*β$^{\Delta 1/\Delta 1}$ knockout and wild-type embryos were used to generate labeled first-strand cDNAs (Cy3 for the wild-type and Cy2 for mutant brains) and hybridized to Incyte cDNA microarrays GEM1 (upper panel) and GEM2 (lower panel). Hybridization intensities of different probes were analyzed using the Rosetta Resolver application. Intensity differences with P values of ≤0.05 were considered differentially expressed and plotted. The $\log_{10}(\text{intensity}^{ko}/\text{intensity}^{wt})$ value (y axis; intensity ratio $[2\beta^{-}/2\beta^{+}]$) was plotted against the $\log_{10}[(\text{intensity}^{ko} + \text{intensity}^{wt})/2]$ value (x axis; average intensity) for each cDNA probe. Examples of differentially expressed genes that are involved in neuronal functions are indicated by arrows.

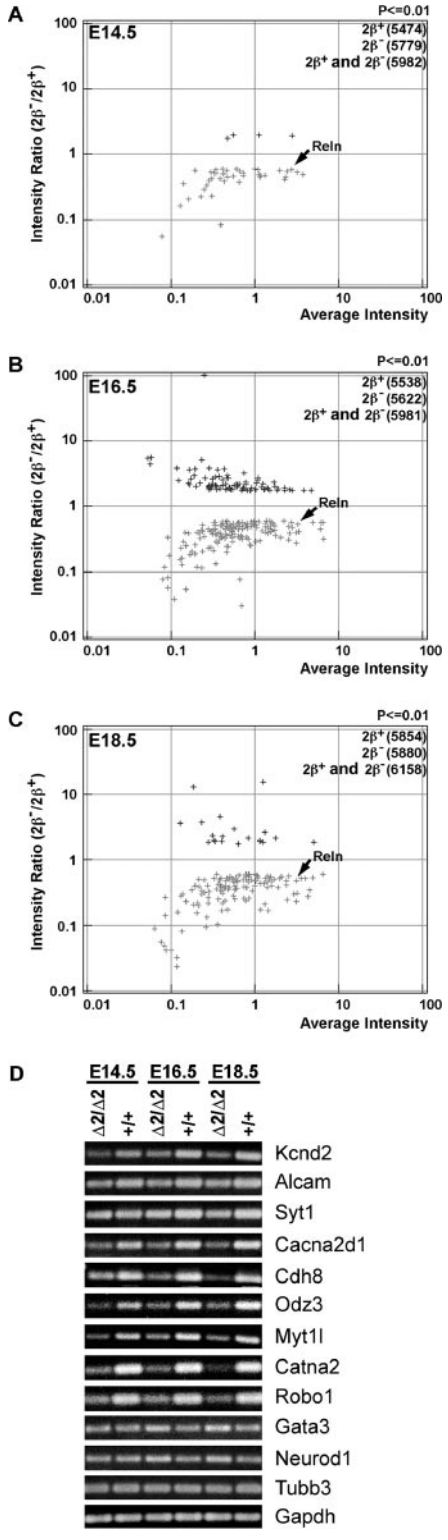

FIG. 2. Differential gene expression in the brains of *top2*$\beta^{\Delta 2/\Delta 2}$ embryos at different developmental stages. (A to C) Transcription profiling of the brains of *top2*$\beta^{\Delta 2/\Delta 2}$ mutant embryos using Affymetrix oligo microarrays. The $\log_{10}$(intensity^{ko}/intensity^{wt}) value (*y* axis; intensity ratio [$2\beta^-/2\beta^+$]) was plotted against the $\log_{10}$[(intensity^{ko} + intensity^{wt})/2] value (*x* axis; average intensity) for each probe set. Probe sets with intensity ratios of ≥1.7-fold (either the intensity^{ko}/intensity^{wt} or intensity^{wt}/intensity^{ko} ratio) and *P* values of ≤0.01 were included in the plot. The numbers of probe sets that are expressed in the brains of wild-type ($2\beta^+$) and *top2*$\beta^{\Delta 2/\Delta 2}$ mutant ($2\beta^-$) embryos as well as the combined unique probe sets ($2\beta^+$ and $2\beta^-$) at each developmental stage are indicated in the upper right hand corner of each plot. (D) RT-PCR analysis of genes that are differentially expressed in the mutant. First-strand cDNAs were reverse transcribed from the total RNAs isolated from *top2*$\beta^{\Delta 2/\Delta 2}$ (Δ2/Δ2) mutant and wild-type (+/+) embryos. PCR was then performed using a primer set specific to each gene as indicated to the right. PCR products were analyzed by agarose gel electrophoresis.

.ncbi.nlm.nih.gov/geo/) and is accessible through the GEO Series query number GSE5458.

RESULTS

Transcription profiling of the brains of *top2*$\beta^{\Delta 1/\Delta 1}$ mutant embryos using cDNA microarrays. cDNA microarray analysis was performed on the brains of E15.5 wild-type and *top2*$\beta^{\Delta 1/\Delta 1}$ embryos (57). Total RNAs were isolated from whole brains (including the olfactory bulb, forebrain, mid-brain, hind brain, and brain stem), and Cy3-labeled (for wild type) or Cy5-labeled (for *top2*$\beta^{\Delta 1/\Delta 1}$) cDNAs were hybridized to the mouse GEM1 and GEM2 arrays (Incyte). Intensity profiles generated from scanning the arrays were uploaded into the Rosetta Resolver system for gene expression data analysis (Rosetta Resolver application; Rosetta Inpharmatics, Inc.). Differentially expressed genes (intensity ratios [Cy5/Cy3] with *P* values of ≤0.05) were recorded (Fig. 1). The full list of the genes that were differentially expressed is shown in Table S1 of the supplemental material. Many of the genes that are involved in neuronal functions, such as *Reln*, *Dab1*, *Catna2*, *Ebf1*, *Pbx3*, *Cacna2d1*, *Ptgds*, *Epha3*, and *Ptprd*, were identified as differentially expressed.

Transcription profiling of the brains of *top2*$\beta^{\Delta 2/\Delta 2}$ mutant embryos using Affymetrix GeneChip microarrays. The interpretation of the above results obtained from *top2*$\beta^{\Delta 1/\Delta 1}$ embryos could be complicated by the presence of the constitutively expressed neomycin resistance gene in the *top2*$\beta^{\Delta 1}$ locus. To avoid this potential complication, all subsequent analyses were performed on the brains of *top2*$\beta^{\Delta 2/\Delta 2}$ embryos in which the truncated *top2*$\beta^{\Delta 2}$ allele did not contain any exogenous DNA sequences.

We collected *top2*$\beta^{\Delta 2/\Delta 2}$ (mutant) and *Top2*$\beta^{+/+}$ (wild-type) embryos at three developmental stages, E14.5, E16.5, and E18.5. Total RNAs from whole brains were isolated. Biotin-labeled cRNAs were then generated and hybridized to the Affymetrix GeneChip microarray MG_U74Av2. This array contains 12,422 probe sets, which include ~6,000 expressed sequence tag clusters and all sequences (~6,000) in the mouse UniGene database (build 74) that have been functionally characterized. Expression profiles of the brains of mouse embryos at different developmental stages were then generated by using the Rosetta Resolver application. There were 5,474, 5,538, and 5,854 probe sets called present in the brains of wild-type E14.5, E16.5, and E18.5 embryos, respectively, and 5,779, 5,622, and 5,880 probe sets in the brains of the *top2*$\beta^{\Delta 2/\Delta 2}$ E14.5, E16.5, and E18.5 embryos, respectively ($P \leq 0.01$) (Fig. 2A to C). The numbers of unique probe sets expressed in wild-type and mutant embryos at E14.5, E16.5, and E18.5 were 5,982, 5,981, and

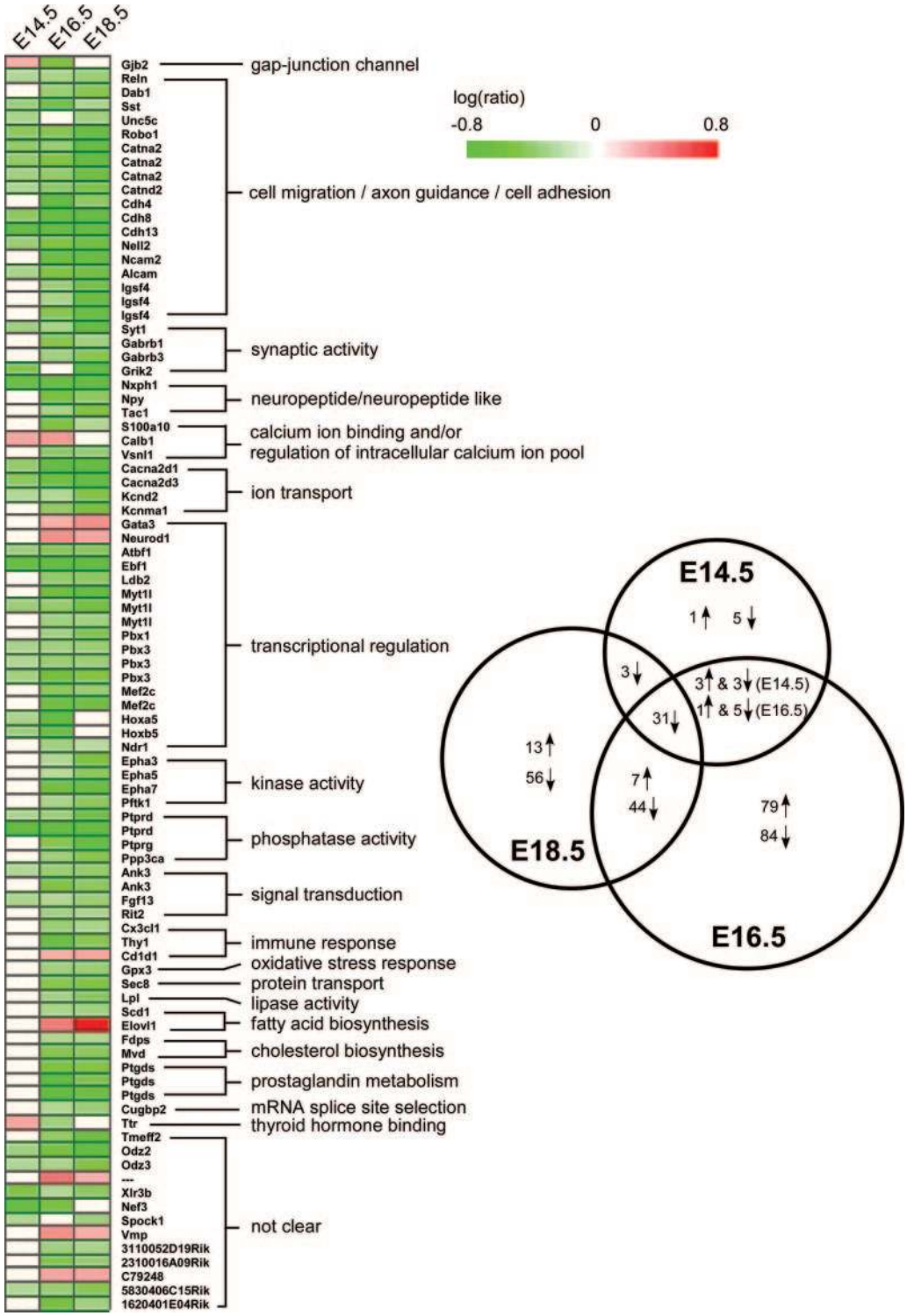

FIG. 3. Genes involved in various biological pathways are affected in the brains of *top2*$\beta^{\Delta 2/\Delta 2}$ mutant embryos. Shown to the right is the Venn diagram representation of the number of overlapping differentially expressed genes in the brains of *top2*$\beta^{\Delta 2/\Delta 2}$ embryos between or among different developmental stages (E14.5, E16.5, and E18.5). ↑, up-regulation; ↓, down-regulation. Shown to the left is a heat map representation of genes showing differential expression at any two (or all three) developmental stages. These genes were grouped together according to their involvement in a particular biological pathway. Each column represents individual developmental stages (E14.5, E16.5, and E18.5). Log(ratio), $\log_{10}(\text{intensity}^{ko}/\text{intensity}^{wt})$; green bar, down-regulation [log(ratio) < 0]; red bar, up-regulation [log(ratio) > 0]; white, no change [log(ratio) $= 0$].

6,158, respectively. We then compared gene expression intensities, using the wild type as the baseline, to generate the ratio intensity data. The distribution of differentially expressed genes at each developmental stage was represented by plotting the intensity ratio ($2\beta^-/2\beta^+$) versus the average intensity (Fig. 2A to C). Differentially expressed probe sets represented 0.77%, 4.2%, and 2.5% of the total expressed genes (5,982, 5,981, and 6,158) at E14.5, E16.5, and E18.5, respectively. Full lists of genes that were differentially expressed at different stages are shown in Tables S2, S3, and S4 in the supplemental material. As shown in Fig. 2A to C, most differentially expressed genes are down-regulated (91, 65, and 87% of the total number of differentially expressed genes at E14.5, E16.5, and E18.5, respectively). As shown previously by Northern hybridization, the steady-state *Reln* message was lower in the brains of *top2*β mutants at E14.5, E16.5, and E18.5 (34). Our microarray approach has also identified *Reln* as one of the down-regulated genes. *Reln* was down-regulated 1.75-, 1.92-, and 2.19-fold at E14.5, E16.5, and E18.5, respectively (Fig. 2A to C).

To confirm the above findings, we performed semiquantitative RT-PCR analysis on some of the differentially expressed genes. As shown in Fig. 2D, genes such as *Kcnd2*, *Alcam*, *Syt1*, *Cacna2d1*, *Cdh8*, *Odz3*, *Myt1l*, *Catna2*, and *Robo1* were down-regulated in *top2*$\beta^{\Delta 2/\Delta 2}$ mutants at all three developmental stages, in agreement with the results obtained from the microarray analysis. In addition, RT-PCR analysis also demonstrated that genes such as *Neurod1* and *Gata3* were up-regulated at both E16.5 and E18.5 (Fig. 2D), again consistent with results obtained from the microarray analysis.

Altered expression of specific neuronal genes in the brains of *top2*$\beta^{\Delta 2/\Delta 2}$ embryos. By comparing the results across three developmental stages, we found 31 probe sets are down-regulated in *top2*$\beta^{\Delta 2/\Delta 2}$ mutant embryos at all three developmental stages (Fig. 3, Venn diagram). This group included genes encoding proteins involved in neuron migration/axon guidance (e.g., *Reln*, *Sst* and *Robo1*), cell adhesion (e.g., *Catna2*, *Catnd2*, *Cdh4*, *Cdh8*, *Nell2*, and *Alcam*), transcription regulation (e.g., *Atbf1*, *Ebf1*, and *Pbx3*), voltage-gated calcium channel activity (e.g., *Cacna2d1* and *Cacna2d3*), and synaptic transmission (e.g., *Syt1*). Some probe sets were differentially expressed at only two developmental stages (a total of 60) (Fig. 3, Venn diagram). For example, *Dab1* (disabled homolog 1), *Gabrb1* and *Gabrb3* (GABA-A receptor subunits beta 1 and beta 3), *Epha3*/*5*/*7* (ephrine receptors), *Ptgds* (prostaglandin D_2 synthase), and *Fdps*/*Mvd* (cholesterol biosynthesis pathway genes) were differentially expressed in *top2*$\beta^{\Delta 2/\Delta 2}$ mutants only at E16.5 and E18.5. These two groups of probe sets were combined (91 in total) and grouped together according to their involvement in various biological pathways, such as cell migration and/or axon guidance, cell adhesion, synaptic activity, ion channeling, kinase and phosphatase activity, transcription regulation, and fatty acid/cholesterol synthesis (Fig. 3, heat map). The majority (greater than 90%) of the genes were down-regulated in *top2*$\beta^{\Delta 2/\Delta 2}$ mutant embryos. However, there were several up-regulated probe sets. They included *Calb1* (calbindin 28K), transcription factors *Gata3* and *Neurod1*, immune response-related antigen *Cd1d*, and *Elovl1* (synthesis of very-long-chain fatty acid).

It is also noteworthy that the results of our cDNA microarray analysis using *top2*$\beta^{\Delta 1/\Delta 1}$ brains are consistent with those using *top2*$\beta^{\Delta 2/\Delta 2}$ brains. For example, *Reln*, *Dab1*, *Catna2*, *Ebf1*, *Pbx3*, *Cacna2d1*, *Ptgds*, *Epha3*, and *Ptprd* were identified as differentially expressed in both studies.

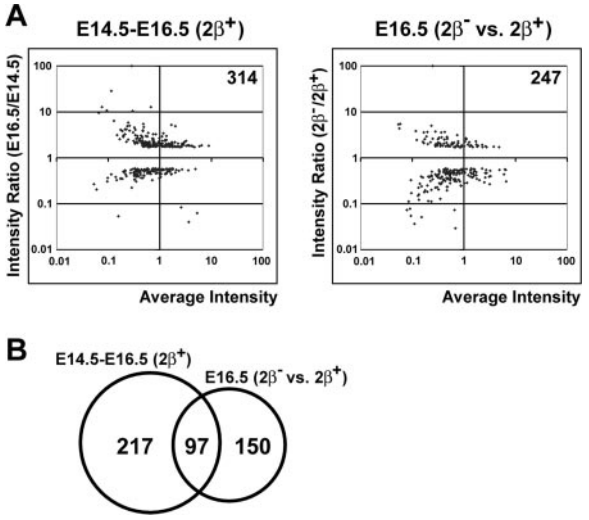

FIG. 4. Developmentally regulated genes are preferentially affected in the brains of *top2*$\beta^{\Delta 2/\Delta 2}$ embryos. (A) Comparison of developmentally regulated genes during normal mouse brain development (E14.5 to E16.5 [$2\beta^+$]) and differentially expressed genes in the brains of mutant embryos (E16.5 [$2\beta^-$ versus $2\beta^+$]). The developmentally regulated genes (E14.5 to E16.5 [$2\beta^+$]) are defined as those that are differentially expressed in the brain of the wild-type E16.5 embryo compared to that of the E14.5 embryo. The $\log_{10}(\text{intensity}^{E16.5}/\text{intensity}^{E14.5})$ value (*y* axis; intensity ratio [E16.5/E14.5]) was plotted against the $\log_{10}[(\text{intensity}^{E14.5} + \text{intensity}^{E16.5})/2]$ value (*x* axis; average intensity) for each probe set. The total number of probe sets that are differentially expressed during this period of development is 314 (intensity ratios ≥ 1.7 [either the intensity $^{E16.5}$/intensity$^{E14.5}$ or intensity$^{E14.5}$/intensity$^{E16.5}$ ratio] and $P \leq 0.01$). The differentially expressed probe sets in the brain of the E16.5 *top2*$\beta^{\Delta 2/\Delta 2}$ mutant embryo are shown to the right (also see similar plot shown in Fig. 2B). (B) Venn diagram representation of the number of overlapping genes between developmentally regulated genes (E14.5 to E16.5 [$2\beta^+$]) and differentially expressed genes (E16.5 [$2\beta^-$ versus $2\beta^+$]).

Developmentally regulated genes are preferentially affected in the brains of *top2*$\beta^{\Delta 2/\Delta 2}$ embryos. As mentioned earlier, the expression of only a small percentage of genes was affected in the brains of *top2*β mutant embryos at different stages of development. However, about one-third of developmentally regulated genes were affected in the *top2*β mutant. Out of 314 developmentally regulated genes (defined as differentially expressed by comparing the expression profiles of the brains of E16.5 and E14.5 wild-type embryos) (Fig. 4A), the expression of 97 (31%) of them was affected in the brain of *top2*$\beta^{\Delta 2/\Delta 2}$ embryos (Fig. 4B). This result indicates that developmentally regulated genes are preferentially affected in *top2*β mutant brains. It should be noted that the expression of the early neuron-specific differentiation marker *Tubb3* (*Tubb3* is expressed in migrating neurons located in the intermediate zone and in some cells in the ventricular zone [9, 28, 36, 37]) was not affected in the cerebral cortex of *top2*β mutants. In addition, the microarray analysis revealed that the expression of growth-related genes (e.g., *Top2*α, thymidylate synthase, and *Cdc2*),

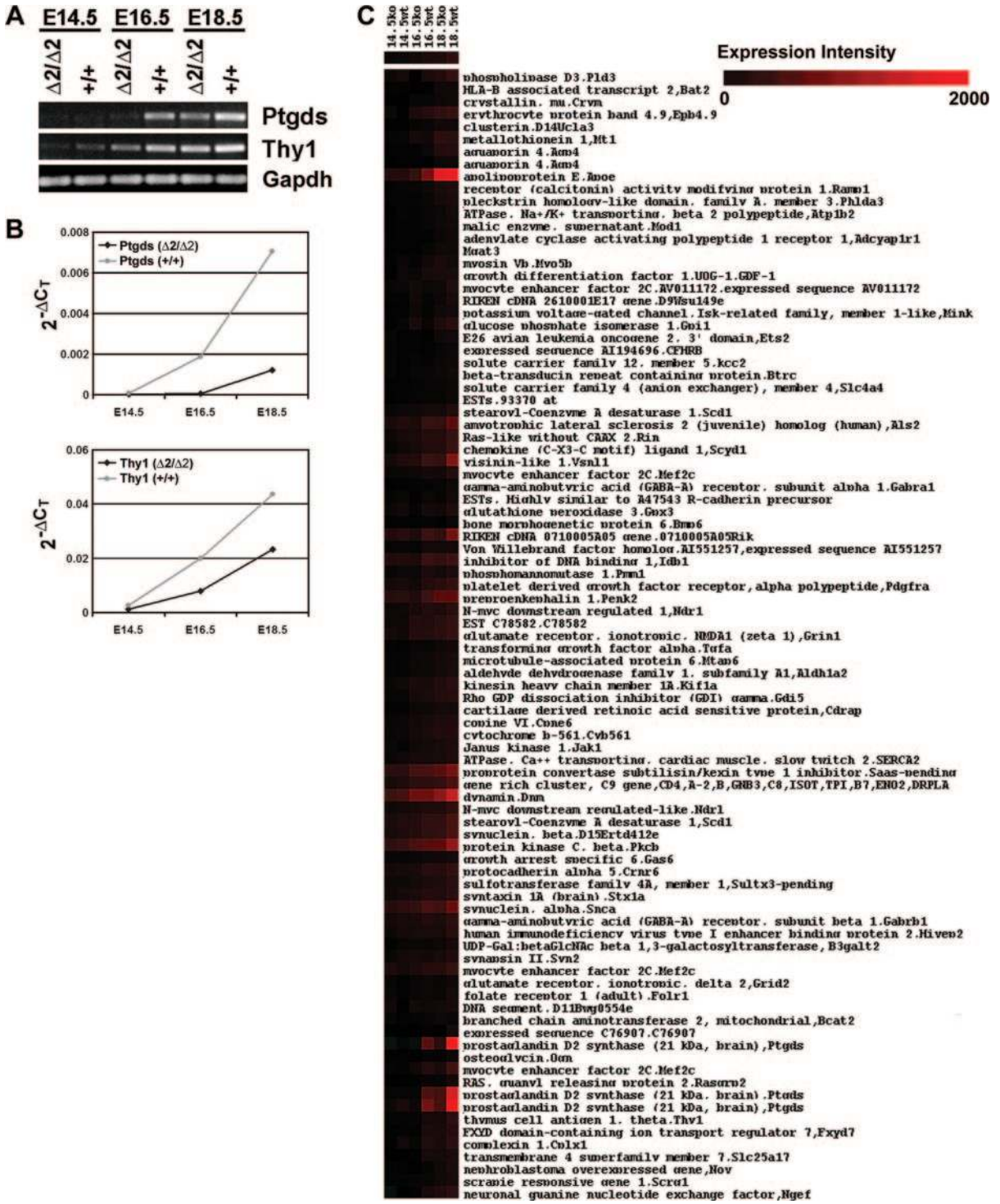

FIG. 5. RT-PCR and clustering analysis of developmentally regulated genes in the brains of *top2*β$^{\Delta 2/\Delta 2}$ embryos. (A) RT-PCR analysis of *Ptgds* and *Thy1* in the brains of *top2*β$^{\Delta 2/\Delta 2}$ mutant embryos. First-strand cDNAs were synthesized using total RNAs isolated from wild-type (+/+) and *top2*β$^{\Delta 2/\Delta 2}$ (Δ2/Δ2) mutant embryos. PCR was then performed using primer pairs specific to *Ptgds* and *Thy1* cDNAs. PCR products were analyzed by agarose gel electrophoresis. (B) Real-time RT-PCR analysis. First-strand cDNAs were used to perform real-time PCR with primer pairs specific to *Ptgds*, *Thy1*, and *Gapdh* cDNAs. The value of the threshold cycle (C_T) for each PCR was determined. The ΔC_T value of *Ptgds* or *Thy1* of wild-type (+/+) or *top2*β mutant (Δ2/Δ2) embryos at a particular developmental stage is defined as the difference between the C_T value of *Ptgds* (or *Thy1*) and that of the corresponding *Gapdh* [C_T (Ptgds or *Thy1*) − C_T (*Gapdh*)]. The $2^{-\Delta CT}$ values for *Ptgds* (upper panel) and *Thy1* (lower panel) were then plotted against each developmental stage (E14.5, E16.5, and E18.5). (C) Heat map plot of hierarchical clustering of absolute expression intensities. Clustering analysis was performed, and a cluster of genes that showed a similar pattern of expression as that of *Ptgds* and *Thy1* is presented. ko, *top2*β$^{\Delta 2/\Delta 2}$; wt, *Top2*β$^{+/+}$.

which are down-regulated during differentiation (7, 11), was not affected in the brains of *top2*β knockout embryos.

RT-PCR analysis was performed on *Ptgds* and *Thy1*, 2 of the 97 developmentally regulated genes that are down-regulated in the E16.5 mutant brain. As shown in Fig. 5A, the expression of both genes in the wild-type brains increased during embryonic development. An increase of expression of these genes was also observed in the mutant brain. However, the expression levels of these genes at all three developmental stages were less than those of the wild-type brain (except for *Ptgds* at E14.5). To confirm this finding, we performed quantitative real-time RT-PCR analysis. As shown in Fig. 5B, *Ptgds* and *Thy1* were induced during development in the brains of *top2*β mutants, although their expression levels were lower than in wild-type embryos. To search for genes with similar expression patterns, we performed a hierarchical clustering analysis on the expression intensities of genes in the brains of mutant and wild-type embryos at E14.5, E16.5, and E18.5. As shown in Fig. 5C, a group of genes showed a similar expression pattern to that of *Ptgds* and *Thy1*. These results suggest that gene activation can still occur in the absence of IIβ, albeit at a reduced rate.

Binding of TopIIβ to IIβ-sensitive genes. To determine whether IIβ is directly involved in transcriptional regulation of specific genes, the binding of IIβ to the 5′ coding and upstream regions of various genes was examined in a ChIP assay. Sheared chromatin with an average size of <4 kb was prepared from E18.5 TOP2β^{+} (two *Top2*β$^{+/+}$ and three *top2*β$^{+/\Delta 2}$ brains pooled together) and *top2*β$^{\Delta 2/\Delta 2}$ brains and immunoprecipitated using anti-TopIIβ antibody. DNAs isolated from the ChIP assay were PCR amplified using primer sets specific to the kb −0.5 region of different genes as described in Materials and Methods. As shown in Fig. 6A, IIβ was detected in the 5′ coding and upstream regions of the IIβ-sensitive genes *Myt1l*, *Cacna2d1*, *Syt1*, *Cdh8*, and *Kcnd2*, but not the IIβ-insensitive gene *Tubb3*, in TOP2β^{+} brains, suggesting a possible direct role of IIβ in the expression of these genes. Interestingly, binding of IIβ to other IIβ-sensitive genes, such as *Ptgds* and *Odz2*, was not detected (Fig. 6A). It is possible that IIβ is either indirectly involved or only transiently involved in the expression of these genes and thus not detectable in the brains of E18.5 embryos. Alternatively, IIβ is bound to a region which is distal to the 5′ region. To obtain more quantitative results, real-time PCR was also performed on DNAs obtained from the ChIP assay described above. The threshold values of PCRs used to amplify the promoter regions of various genes (e.g., *Cacna2d1*, *Syt1*, *Kcnd2*, and *Tubb3*) in the immunoprecipitated (by IIβ-specific antibody) chromatin were first normalized to those of the "input" and then divided by the normalized "control" (no antibody was added during ChIP) using the $2^{-\Delta\Delta CT}$ method (32). As shown in Fig. 6B, four- to sevenfold more DNAs corresponding to the 5′ coding and upstream regions of *Cacna2d1*, *Syt1*, and *Kcnd2* were brought down by IIβ-specific antibody than "controls" in the TOP2β^{+} sample. By contrast, no IIβ association with the 5′ region of *Tubb3* (a IIβ-insensitive gene) was demonstrable.

Fine mapping of TopIIβ binding was performed on a IIβ-sensitive gene, *Kcnd2*, using cross-linked chromatin with an average size of 300 bp (Fig. 6C, inset). As shown in Fig. 6C (see primer sets at positions kb −19.6, −5, −2.5, −0.5, +2.5, +10, and +503.55 of the transcription unit), IIβ binding was detected within the entire transcription unit (about 513 kb) of the *Kcnd2* gene, with the highest binding found near the promoter region (kb −0.5 to +2.5). By contrast, no IIβ binding was detected in the upstream region of the *Kcnd2* gene at kb −2.5 and −5 (Fig. 6C). However, IIβ binding was detected at kb −19.6. These results provide further support for a role of TopIIβ in the transcription of the IIβ-sensitive genes.

Coregulated expression pattern of TopIIβ and HDAC2 in the developing mouse cerebral cortex. It has been shown that TopIIβ interacts with class I histone deacetylases, HDAC1 and HDAC2, in cultured cells (23, 45). HDAC1 and HDAC2 are subunits of the chromatin remodeling complex NurD (56). Their interaction with IIβ may suggest a role for IIβ in chromatin remodeling. Because the overall expression level of HDAC1 is much lower than that of HDAC2 in the brain (data not shown), we only analyzed the expression pattern of HDAC2. As shown in Fig. 7A, the expression pattern of HDAC2 (right panel; stained with rabbit anti-HDAC2 antibody) was surprisingly similar to that of IIβ (left panel; stained with rabbit anti-IIβ antibody) in the cerebral cortex of the E14.5 *top2*β$^{+/\Delta 2}$ mouse embryo. Both HDAC2 and IIβ were found to be much elevated in the postmitotic (nonproliferating) neurons located in the cortical plate. Neurons in the cortical plate are known to represent progressively more mature neurons along the neuronal differentiation pathway. By contrast, very few cells were found to express HDAC2 and IIβ in the intermediate zone, where less-mature postmitotic neurons are located, or in the ventricular zone, where neuronal precursors are located. To confirm the coregulated expression of IIβ and HDAC2 in postmitotic cortical neurons, coimmunostaining of E14.5 *top2*β$^{+/\Delta 2}$ brain sections using both rabbit anti-IIβ and mouse anti-HDAC2 antibodies was performed. As shown in Fig. 7B (merged images at three magnifications, ×1, ×2, and ×4), IIβ and HDAC2 were coexpressed in postmitotic neurons located in the cortical plate region.

A similar analysis was performed on wild-type E18.5 brain sections. Again, HDAC2 and IIβ were found to be expressed in a similar pattern (Fig. 7C). Both were expressed at higher levels in the region spanning the marginal zone, the cortical plate, and the subplate. Their expression in the intermediate zone and the ventricular zone was much lower (Fig. 7C). In addition, HDAC2 was found to be expressed at higher levels in cells occupying the more superficial layers of the cortex in the E18.5 *top2*β$^{\Delta 2/\Delta 2}$ embryo (Fig. 7C). Expression in other regions (i.e., intermediate and ventricular zones) of the cortex was low (Fig. 7C). The superficial layers of the E18.5 *top2*β$^{\Delta 2/\Delta 2}$ cortical plate were known to be occupied by early-borne neurons (i.e., neurons at a more mature state compared to neurons located in the deeper regions of the cortical plate of the *top2*β$^{\Delta 2/\Delta 2}$ cortex) (34). These results suggest that HDAC2 and IIβ are preferentially expressed in more mature neurons which are in their later stages of differentiation.

DISCUSSION

A previous macroarray study (with 300 cDNA probes) using ICRF-193 (a TopII-specific inhibitor) in isolated rat cerebellar granule neurons demonstrated that the expression of many neuronal genes is altered (48). However, the use of ICRF-193 for studying the function of TopIIβ in neurons could have

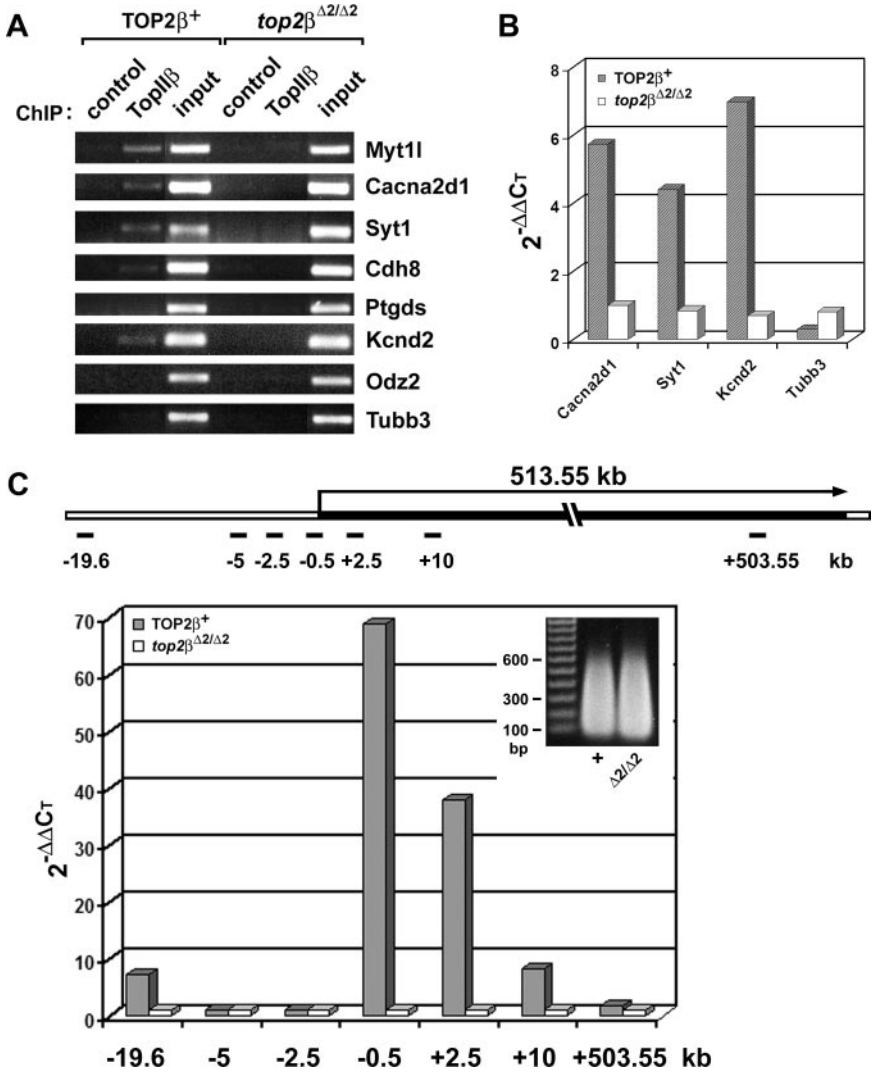

FIG. 6. ChIP analysis of TopIIβ binding to TopIIβ-sensitive genes. (A) ChIP analysis using PCR. ChIP analysis using anti-TopIIβ antibody was performed on sheared chromatin (<4 kb) isolated from E18.5 brains of both TOP2β^{+} (two *Top2*β$^{+/+}$ and three *top2*β$^{\Delta 2/\Delta 2}$ brains combined) and null mutant (*top2*β$^{\Delta 2/\Delta 2}$) embryos. The ChIP products were PCR amplified using primer sets corresponding to the promoter regions of various genes (*Myt1l*, *Cacna2d1*, *Syt1*, *Cdh8*, *Ptgds*, *Kcnd2*, *Odz2*, and *Tubb3*) as described in Materials and Methods. For control samples, no antibody was added during ChIP. (B) ChIP analysis using quantitative real-time PCR. Quantitative real-time PCR was performed on the same ChIP products (described for panel A) using the same primer sets corresponding to the promoter regions of *Cacna2d1*, *Syt1*, *Kcnd2*, and *Tubb3*. Data were analyzed using the SDS 2.2 software. The threshold cycle value for each sample was chosen from the linear range. The relative amount of DNA in the ChIP product was calculated with the use of the $2^{-\Delta\Delta CT}$ method (32), using "input" as the normalization standard for each sample and the "control" as the baseline. (C) TopIIβ binding to the transcription unit of the *Kcnd2* gene. Quantitative real-time PCR was performed on ChIP products as described for panel B, except that the ChIP was performed on sheared chromatin with an average size of 300 bp (insert) and the primer sets covering different regions of the *Kcnd2* gene (see the schematic representation of the 513.55-kb transcription unit of the *Kcnd2* gene) were used.

potential problems for two reasons. First, ICRF-193 can cause a gain-of-function effect by trapping TopII into circular clamps on chromatin which impede the movement of elongating RNA polymerases (54). Consequently, alteration of gene expression by ICRF-193 treatment may not indicate an involvement of TopII in gene expression. Second, ICRF-193 inhibits both TopIIα and TopIIβ. It is unclear whether it is TopIIβ or the residual TopIIα that is responsible for the ICRF-193 effect on gene expression. Our current large-scale microarray analysis has revealed interesting features of the gene expression profiles in the brains of *top2*β knockout embryos. First, the expression of only a very small fraction of genes (0.73, 4.2, and 2.7%, respectively, at E14.5, E16.5, and E18.5) are affected in *top2*β mutants. For example, the expression of genes encoding proteins involved in neuron migration (e.g., *Reln*, *Dab1*, *Sst*, and *Robo1*), cell adhesion (e.g., *Catna2*, *Cdh4*, *Cdh8*, *Nell2*, and *Alcam*), voltage-gated calcium channel activity (e.g., *Cacna2d1* and *Cacna2d3*), and synaptic transmission (e.g., *Syt1*) was down-regulated in the mutant. Down-regulation of some of these genes may be in part responsible for the neuronal migration defect observed in the developing cortex of *top2*β mutant embryos (34). The expression of some transcription

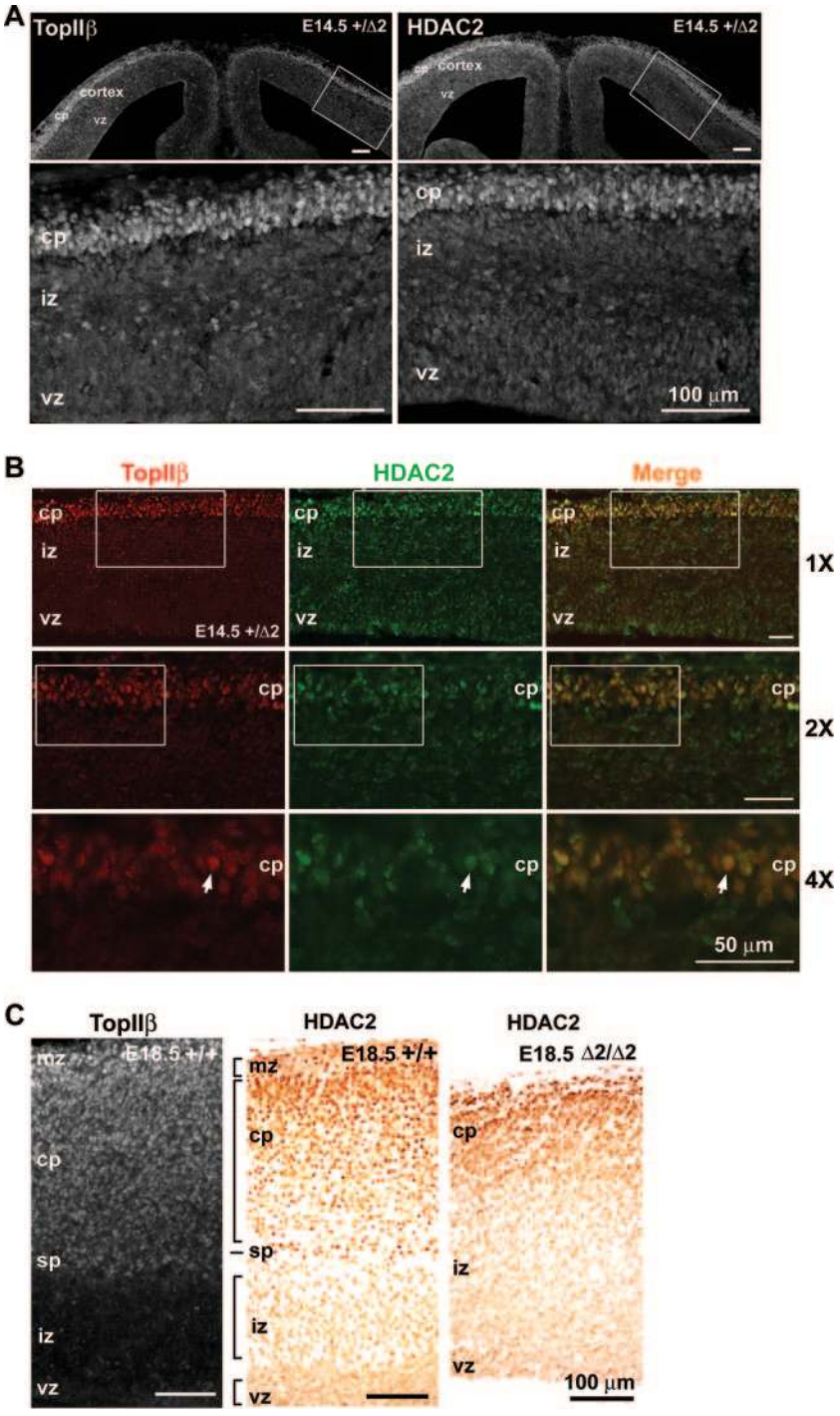

FIG. 7. Elevated expression of TopIIβ and HDAC2 in more-mature neurons of the cerebral cortex. (A) Coronal sections (20-μm cryosections) of the E14.5 *top2*$\beta^{+/\Delta 2}$ telencephalon immunostained with antibodies against IIβ (left panel) and HDAC2 (right panel). The lower panels represent the magnified views of the boxed areas in the corresponding upper panels. (B) Coronal sections (16-μm cryosections) of the E14.5 *top2*$\beta^{+/\Delta 2}$ medial lateral telencephalon immunostained with antibodies against IIβ (red) and HDAC2 (green). The 2× magnification images of the boxed areas of the top panels (labeled 1X) are shown in the middle panels, and 2× magnification images (labeled 4X) of the boxed areas of the middle panels are shown in the bottom panels. A representative neuron with colocalized IIβ (red) and HDAC2 (green) is indicated by an arrow. The relative magnifications (×1, ×2, and ×4) are shown on the right of the panels. (C) E18.5 sagittal sections of the *Top2*$\beta^{+/+}$ neocortex stained with anti-IIβ (20-μm cryosection) and anti-HDAC2 (6-μm paraffin section) antibodies, as well as the E18.5 sagittal section of the *top2*$\beta^{\Delta 2/\Delta 2}$ neocortex stained with anti-HDAC2 antibody (6-μm paraffin section). Bars, 100 μm (A and C) and 50 μm (B). vz, ventricular zone; iz, intermediate zone; sp, subplate; cp, cortical plate; mz, marginal zone.

factors (e.g., *Myt1l*, *Ebf1*, and *Mef2c*) was also down-regulated, while that of others (e.g., *Gata3* and *Neurod1*) was up-regulated in *top2*β mutants. Many of these transcription factors have been implicated in various differentiation pathways (1, 15, 27, 39, 42). The fact that the expression of certain transcription factors is affected in *top2*β mutants suggests the possibility that the altered expression of at least some of the differentially expressed genes may be an indirect effect of *top2*β deletion. Second, the expression of nearly one-third of the developmentally regulated genes was either up-regulated (e.g., *Matr3* and *Cas1*) or down-regulated (e.g., *Cdh13*, *Ptgds*, and *Thy1*) in *top2*β mutants. Interestingly, the expression of general housekeeping genes (i.e., genes involved in cell proliferation, protein synthesis, and transcription, for example, *Top2*α, *Cdc2*, *Rbp1*, *Rpo1-2*, and *Rpb1*) is not affected. These results indicate that IIβ is specifically required for the proper expression of a group of developmentally regulated genes.

Our microarray studies have also demonstrated that the expression of early differentiation markers does not appear to be affected. For example, the expression of the early neuronal differentiation marker *Tubb3* (9) was not affected in the brains of *top2*β mutant embryos. *Tubb3* is known to be an early differentiation marker which is expressed immediately after the last cell division (28, 36, 37). Furthermore, the expression of genes (e.g., *Top2*α and the thymidylate synthase gene) encoding general cell proliferation markers that are down-regulated during terminal differentiation (7, 11) was not affected. The effect of IIβ on the expression of late differentiation markers is consistent with its expression pattern in the marginal zone, cortical plate, and subplate but not the intermediate zone or the ventricular zone. Neurons in the marginal zone, cortical plate, and subplate are known to be at later stages of differentiation than neurons in the intermediate zone and ventricular zone. IIα is known to have an opposite expression pattern compared to IIβ in the developing cortex. IIα is expressed abundantly in proliferating neuronal precursors. Its expression is very low in other regions of the brain where postmitotic neurons are located (46, 52). It is possible that IIα and IIβ may have overlapping functions in gene expression. The expression of early differentiation markers may require IIα, while that of late markers requires IIβ. Consequently, IIβ deletion does not affect early differentiation programming but does affect the expression of many developmentally regulated genes at later stages of terminal differentiation. In addition, our studies on the expression of *Ptgds* and *Thy1* genes at different stages of brain development have demonstrated that both genes can still be induced in *top2*β null mutants, albeit at a reduced rate, suggesting that IIβ is important but not essential for the activation of these genes. It is possible that alternative mechanisms may exist to enable the expression of these genes in the absence of IIβ. For example, in the absence of IIβ, the expression of these genes may depend on either residual IIα and/or TopI.

The ChIP analysis demonstrated a direct interaction between IIβ and the 5′ coding and upstream regions of a number of IIβ-sensitive genes (e.g., *Myt1l*, *Cacna2d1*, *Syt1*, and *Kcnd2*), suggesting a possible direct role of IIβ in the transcription of these genes. Based on the known catalytic activity of IIβ, it is reasonable to speculate that IIβ may be involved in transcription initiation, elongation, or both. The potential role of IIβ in transcription elongation is conceptually easier to understand in the framework of the twin-domain model of transcription (31). Indeed, fine mapping of TopIIβ binding by ChIP has demonstrated the presence of TopIIβ in the transcription unit of a IIβ-sensitive gene, *Kcnd2* (Fig. 6C). This result is consistent with results from a recent publication in which TopIIβ was shown to bind to the pS2 promoter and stimulate transcription in 17β-estradiol-treated MCF-7 cells (24). However, our transcriptional profiling studies in developing brains have demonstrated that only a small percentage of expressed genes are affected in *top2*β null embryos. It seems unlikely that TopIIβ is involved in transcription elongation of all genes. One possibility is that TopIIβ is only involved in the transcription elongation of IIβ-sensitive genes. It is well documented that TopI is specifically located within the transcribed regions of many genes (16, 38, 43, 59). The precise roles of TopI and TopIIβ in transcription elongation of different genes remain to be established.

We have also considered the possibility that TopIIβ is involved in transcription initiation. IIβ may affect transcription initiation through its generation of negative superhelical tension in a loop domain spanning the gene/promoter. This possibility could be supported by the report that the *Drosophila melanogaster Hsp70* gene locus (and presumably other microdomains) is under negative superhelical tension regardless of its transcription status (25). Using a Me3-psoralen photobinding assay, random integration of the hygromycin B phosphotransferase (*Hph*) gene into different chromosomal domains has also indicated various levels of unconstrained negative supercoiling (26). However, IIβ itself does not exhibit any detectable supercoiling activity in vitro. Alternatively, IIβ is involved in local chromatin reorganization to enable activation/repression of developmentally regulated genes. Such a possibility could be supported by circumstantial evidence. First, a role for TopII in chromosome condensation/decondensation has been suggested (12, 50, 53). It is plausible that IIα is more specialized for large-scale chromosome-wide condensation/decondensation in proliferating cells, while IIβ is more specialized for local/regional chromatin condensation/decondensation in nonproliferating or differentiated cells. Second, TopII has been shown to interact with condensin (4, 33), histone deacetylases HDAC1 and HDAC2 (23, 45), and chromatin remodeling factors (30). It is noteworthy that human IIβ, but not IIα, can be copurified with the chromatin remodeling factor ACF (30). Our current studies have also demonstrated a similar temporal-spatial expression pattern of TopIIβ and HDAC2 in developing neurons. While the interaction of IIβ with HDACs may indicate a role for IIβ in gene repression, its interaction with chromatin remodeling complexes could suggest a role in gene activation. Consequently, IIβ may play a role in both gene activation and repression. Third, studies on the chicken β-globin locus have demonstrated that most DNase I-hypersensitive sites are TopII cleavage sites, suggesting an association between TopII and gene activation (40). The association of TopII with the MAR/SAR sequences could also suggest a role of TopII in chromatin structural organization and the control of the topology of chromosomal loop domains (5, 40, 44). TopII has been suggested to be located at the base of chromosomal DNA loops. It seems possible that TopIIβ may perform its function through controlling the topology of the loop domains and thus influencing chromatin dynamics

and gene expression. It is noteworthy that we have observed binding of TopIIβ to the kb −19.6 region of the *Kcnd2* gene. It remains to be determined whether this region contains a DNase I-hypersensitive site(s) and/or MAR/SAR site(s).

The interaction of TopII with condensin is of particular interest. Recent studies have suggested condensin is involved not only in chromosome condensation/decondensation during mitosis but also in other functions, such as gene expression (17, 19, 29, 35). In fact, it has been suggested that condensin affects gene expression through its influences on control mechanisms that operate globally at a chromosome-wide level, regionally over a subchromosomal domain, or locally on an individual gene (17). For example, the *Drosophila* TopII interacts with Barren (BARR, a CAP-H homolog of condensin I) and binds to the Polycomb group (PcG) target sequences in the bithorax complex (33). In addition, the PcG protein Polyhomeotic interacts physically with TopII and BARR, and BARR is required for Fab-7-regulated homeotic gene expression (33). Another interesting example is from the recent report that links condensin to the bookmarking of the active chromatin state of the *hsp70i* gene (55). It was shown that the active chromatin state of the *hsp70i* gene is initiated by the binding of the transcription factor HSF2, which leads to inactivation (through the recruitment of protein phosphatase 2A) of the condensin complexes in its vicinity and hence decompaction of the chromatin in the locus (55). It seems plausible that TopIIβ, together with condensin and/or other chromatin remodeling complexes, may play a role in local/regional chromatin reorganization and thus impact gene expression.

ACKNOWLEDGMENTS

We are grateful to J. Couget, P. Grosu, and R. Gali for their assistance in microarray processing and data analysis at the Bauer Center for Genomic Research of Harvard University. We also thank F. Boege for providing the anti-TopIIβ antibody and L. Wood for reading the manuscript.

This work was supported by NIH RO1 grants GM24544 (J.C.W.), CA102463 (L.F.L.), and CA39662 (L.F.L.).

REFERENCES

1. **Allen, M. P., M. Xu, C. Zeng, S. A. Tobet, and M. E. Wierman.** 2000. Myocyte enhancer factors-2B and -2C are required for adhesion related kinase repression of neuronal gonadotropin releasing hormone gene expression. J. Biol. Chem. **275:**39662–39670.
2. **Austin, C. A., and K. L. Marsh.** 1998. Eukaryotic DNA topoisomerase II beta. Bioessays **20:**215–226.
3. **Austin, C. A., J. H. Sng, S. Patel, and L. M. Fisher.** 1993. Novel HeLa topoisomerase II is the II beta isoform: complete coding sequence and homology with other type II topoisomerases. Biochim. Biophys. Acta **1172:** 283–291.
4. **Bhat, M. A., A. V. Philp, D. M. Glover, and H. J. Bellen.** 1996. Chromatid segregation at anaphase requires the barren product, a novel chromosome-associated protein that interacts with topoisomerase II. Cell **87:**1103–1114.
5. **Boulikas, T.** 1995. Chromatin domains and prediction of MAR sequences. Int. Rev. Cytol. **162A:**279–388.
6. **Capranico, G., S. Tinelli, C. A. Austin, M. L. Fisher, and F. Zunino.** 1992. Different patterns of gene expression of topoisomerase II isoforms in differentiated tissues during murine development. Biochim. Biophys. Acta **1132:**43–48.
7. **Chen, Y., J. A. Sokoloski, E. Chu, and A. C. Sartorelli.** 1998. Regulation of the expression of enzymes involved in the replication of DNA in chemically induced monocytic/macrophagic differentiation of HL-60 leukemia cells. Leuk. Res. **22:**697–703.
8. **Cuvier, O., and T. Hirano.** 2003. A role of topoisomerase II in linking DNA replication to chromosome condensation. J. Cell Biol. **160:**645–655.
9. **Del Rio, J. A., A. Martinez, C. Auladell, and E. Soriano.** 2000. Developmental history of the subplate and developing white matter in the murine neocortex. Neuronal organization and relationship with the main afferent systems at embryonic and perinatal stages. Cereb. Cortex **10:**784–801.
10. **DiNardo, S., K. Voelkel, and R. Sternglanz.** 1984. DNA topoisomerase II mutant of Saccharomyces cerevisiae: topoisomerase II is required for segregation of daughter molecules at the termination of DNA replication. Proc. Natl. Acad. Sci. USA **81:**2616–2620.
11. **Dobashi, Y., M. Shoji, M. Kitagawa, T. Noguchi, and T. Kameya.** 2000. Simultaneous suppression of cdc2 and cdk2 activities induces neuronal differentiation of PC12 cells. J. Biol. Chem. **275:**12572–12580.
12. **Downes, C. S., D. J. Clarke, A. M. Mullinger, J. F. Gimenez-Abian, A. M. Creighton, and R. T. Johnson.** 1994. A topoisomerase II-dependent G_2 cycle checkpoint in mammalian cells. Nature **372:**467–470.
13. **Drake, F. H., J. P. Zimmerman, F. L. McCabe, H. F. Bartus, S. R. Per, D. M. Sullivan, W. E. Ross, M. R. Mattern, R. K. Johnson, S. T. Crooke, et al.** 1987. Purification of topoisomerase II from amsacrine-resistant P388 leukemia cells. Evidence for two forms of the enzyme. J. Biol. Chem. **262:**16739–16747.
14. **Eisen, M. B., P. T. Spellman, P. O. Brown, and D. Botstein.** 1998. Cluster analysis and display of genome-wide expression patterns. Proc. Natl. Acad. Sci. USA **95:**14863–14868.
15. **Garel, S., F. Marin, R. Grosschedl, and P. Charnay.** 1999. Ebf1 controls early cell differentiation in the embryonic striatum. Development **126:**5285–5294.
16. **Gilmour, D. S., and S. C. Elgin.** 1987. Localization of specific topoisomerase I interactions within the transcribed region of active heat shock genes by using the inhibitor camptothecin. Mol. Cell. Biol. **7:**141–148.
17. **Hagstrom, K. A., and B. J. Meyer.** 2003. Condensin and cohesin: more than chromosome compactor and glue. Nat. Rev. Genet. **4:**520–534.
18. **Heck, M. M., W. N. Hittelman, and W. C. Earnshaw.** 1988. Differential expression of DNA topoisomerases I and II during the eukaryotic cell cycle. Proc. Natl. Acad. Sci. USA **85:**1086–1090.
19. **Hirano, T., R. Kobayashi, and M. Hirano.** 1997. Condensins, chromosome condensation protein complexes containing XCAP-C, XCAP-E and a Xenopus homolog of the Drosophila Barren protein. Cell **89:**511–521.
20. **Holm, C., T. Goto, J. C. Wang, and D. Botstein.** 1985. DNA topoisomerase II is required at the time of mitosis in yeast. Cell **41:**553–563.
21. **Holm, C., T. Stearns, and D. Botstein.** 1989. DNA topoisomerase II must act at mitosis to prevent nondisjunction and chromosome breakage. Mol. Cell. Biol. **9:**159–168.
22. **Hsiang, Y. H., H. Y. Wu, and L. F. Liu.** 1988. Proliferation-dependent regulation of DNA topoisomerase II in cultured human cells. Cancer Res. **48:**3230–3235.
23. **Johnson, C. A., K. Padget, C. A. Austin, and B. M. Turner.** 2001. Deacetylase activity associates with topoisomerase II and is necessary for etoposide-induced apoptosis. J. Biol. Chem. **276:**4539–4542.
24. **Ju, B. G., V. V. Lunyak, V. Perissi, I. Garcia-Bassets, D. W. Rose, C. K. Glass, and M. G. Rosenfeld.** 2006. A topoisomerase IIβ-mediated dsDNA break required for regulated transcription. Science **312:**1798–1802.
25. **Jupe, E. R., R. R. Sinden, and I. L. Cartwright.** 1993. Stably maintained microdomain of localized unrestrained supercoiling at a Drosophila heat shock gene locus. EMBO J. **12:**1067–1075.
26. **Kramer, P. R., and R. R. Sinden.** 1997. Measurement of unrestrained negative supercoiling and topological domain size in living human cells. Biochemistry **36:**3151–3158.
27. **Lee, J. E., S. M. Hollenberg, L. Snider, D. L. Turner, N. Lipnick, and H. Weintraub.** 1995. Conversion of Xenopus ectoderm into neurons by NeuroD, a basic helix-loop-helix protein. Science **268:**836–844.
28. **Lee, M. K., J. B. Tuttle, L. I. Rebhun, D. W. Cleveland, and A. Frankfurter.** 1990. The expression and posttranslational modification of a neuron-specific beta-tubulin isotype during chick embryogenesis. Cell Motil. Cytoskeleton **17:**118–132.
29. **Legagneux, V., F. Cubizolles, and E. Watrin.** 2004. Multiple roles of Condensins: a complex story. Biol. Cell **96:**201–213.
30. **LeRoy, G., A. Loyola, W. S. Lane, and D. Reinberg.** 2000. Purification and characterization of a human factor that assembles and remodels chromatin. J. Biol. Chem. **275:**14787–14790.
31. **Liu, L. F., and J. C. Wang.** 1987. Supercoiling of the DNA template during transcription. Proc. Natl. Acad. Sci. USA **84:**7024–7027.
32. **Livak, K. J., and T. D. Schmittgen.** 2001. Analysis of relative gene expression data using real-time quantitative PCR and the $2^{-\Delta\Delta CT}$ method. Methods **25:**402–408.
33. **Lupo, R., A. Breiling, M. E. Bianchi, and V. Orlando.** 2001. Drosophila chromosome condensation proteins topoisomerase II and Barren colocalize with Polycomb and maintain Fab-7 PRE silencing. Mol. Cell **7:**127–136.
34. **Lyu, Y. L., and J. C. Wang.** 2003. Aberrant lamination in the cerebral cortex of mouse embryos lacking DNA topoisomerase IIβ. Proc. Natl. Acad. Sci. USA **100:**7123–7128.
35. **Machin, F., K. Paschos, A. Jarmuz, J. Torres-Rosell, C. Pade, and L. Aragon.** 2004. Condensin regulates rDNA silencing by modulating nucleolar Sir2p. Curr. Biol. **14:**125–130.
36. **Menezes, J. R., and M. B. Luskin.** 1994. Expression of neuron-specific tubulin defines a novel population in the proliferative layers of the developing telencephalon. J. Neurosci. **14:**5399–5416.
37. **Moody, S. A., M. S. Quigg, and A. Frankfurter.** 1989. Development of the

peripheral trigeminal system in the chick revealed by an isotype-specific anti-beta-tubulin monoclonal antibody. J. Comp. Neurol. **279:**567–580.
38. **Ness, P. J., R. W. Parish, and T. Koller.** 1986. Mapping of endogenous nuclease-sensitive regions and of putative topoisomerase sites of action along the chromatin of Dictyostelium ribosomal RNA genes. J. Mol. Biol. **188:**287–300.
39. **Pata, I., M. Studer, J. H. van Doorninck, J. Briscoe, S. Kuuse, J. D. Engel, F. Grosveld, and A. Karis.** 1999. The transcription factor GATA3 is a downstream effector of Hoxb1 specification in rhombomere 4. Development **126:**5523–5531.
40. **Reitman, M., and G. Felsenfeld.** 1990. Developmental regulation of topoisomerase II sites and DNase I-hypersensitive sites in the chicken beta-globin locus. Mol. Cell. Biol. **10:**2774–2786.
41. **Rice, D. S., and T. Curran.** 2001. Role of the reelin signaling pathway in central nervous system development. Annu. Rev. Neurosci. **24:**1005–1039.
42. **Romm, E., J. A. Nielsen, J. G. Kim, and L. D. Hudson.** 2005. Myt1 family recruits histone deacetylase to regulate neural transcription. J. Neurochem. **93:**1444–1453.
43. **Stewart, A. F., R. E. Herrera, and A. Nordheim.** 1990. Rapid induction of c-fos transcription reveals quantitative linkage of RNA polymerase II and DNA topoisomerase I enzyme activities. Cell **60:**141–149.
44. **Strick, R., and U. K. Laemmli.** 1995. SARs are cis DNA elements of chromosome dynamics: synthesis of a SAR repressor protein. Cell **83:**1137–1148.
45. **Tsai, S. C., N. Valkov, W. M. Yang, J. Gump, D. Sullivan, and E. Seto.** 2000. Histone deacetylase interacts directly with DNA topoisomerase II. Nat. Genet. **26:**349–353.
46. **Tsutsui, K., O. Hosoya, K. Sano, and A. Tokunaga.** 2001. Immunohistochemical analyses of DNA topoisomerase II isoforms in developing rat cerebellum. J. Comp. Neurol. **431:**228–239.
47. **Tsutsui, K., S. Okada, M. Watanabe, T. Shohmori, S. Seki, and Y. Inoue.** 1993. Molecular cloning of partial cDNAs for rat DNA topoisomerase II isoforms and their differential expression in brain development. J. Biol. Chem. **268:**19076–19083.
48. **Tsutsui, K., K. Sano, A. Kikuchi, and A. Tokunaga.** 2001. Involvement of DNA topoisomerase IIβ in neuronal differentiation. J. Biol. Chem. **276:** 5769–5778.
49. **Turley, H., M. Comley, S. Houlbrook, N. Nozaki, A. Kikuchi, I. D. Hickson, K. Gatter, and A. L. Harris.** 1997. The distribution and expression of the two isoforms of DNA topoisomerase II in normal and neoplastic human tissues. Br. J. Cancer **75:**1340–1346.
50. **Uemura, T., H. Ohkura, Y. Adachi, K. Morino, K. Shiozaki, and M. Yanagida.** 1987. DNA topoisomerase II is required for condensation and separation of mitotic chromosomes in S. pombe. Cell **50:**917–925.
51. **Wang, J. C.** 2002. Cellular roles of DNA topoisomerases: a molecular perspective. Nat. Rev. Mol. Cell Biol. **3:**430–440.
52. **Watanabe, M., K. Tsutsui, and Y. Inoue.** 1994. Differential expressions of the topoisomerase II alpha and II beta mRNAs in developing rat brain. Neurosci. Res. **19:**51–57.
53. **Wood, E. R., and W. C. Earnshaw.** 1990. Mitotic chromatin condensation in vitro using somatic cell extracts and nuclei with variable levels of endogenous topoisomerase II. J. Cell Biol. **111:**2839–2850.
54. **Xiao, H., Y. Mao, S. D. Desai, N. Zhou, C. Y. Ting, J. Hwang, and L. F. Liu.** 2003. The topoisomerase IIβ circular clamp arrests transcription and signals a 26S proteasome pathway. Proc. Natl. Acad. Sci. USA **100:**3239–3244.
55. **Xing, H., D. C. Wilkerson, C. N. Mayhew, E. J. Lubert, H. S. Skaggs, M. L. Goodson, Y. Hong, O. K. Park-Sarge, and K. D. Sarge.** 2005. Mechanism of hsp70i gene bookmarking. Science **307:**421–423.
56. **Xue, Y., J. Wong, G. T. Moreno, M. K. Young, J. Cote, and W. Wang.** 1998. NURD, a novel complex with both ATP-dependent chromatin-remodeling and histone deacetylase activities. Mol. Cell **2:**851–861.
57. **Yang, X., W. Li, E. D. Prescott, S. J. Burden, and J. C. Wang.** 2000. DNA topoisomerase IIβ and neural development. Science **287:**131–134.
58. **Yue, H., P. S. Eastman, B. B. Wang, J. Minor, M. H. Doctolero, R. L. Nuttall, R. Stack, J. W. Becker, J. R. Montgomery, M. Vainer, and R. Johnston.** 2001. An evaluation of the performance of cDNA microarrays for detecting changes in global mRNA expression. Nucleic Acids Res. **29:**E41.
59. **Zhang, H., J. C. Wang, and L. F. Liu.** 1988. Involvement of DNA topoisomerase I in transcription of human ribosomal RNA genes. Proc. Natl. Acad. Sci. USA **85:**1060–1064.